

Supporting Information

Guest-Tuned Proton Conductivity of Porphyrinylphosphonate-Based Hydrogen-Bonded Organic Frameworks

Yijie Wang,^a Jianbo Yin,^a Di Liu,^a Chengqi Gao,^a Zixi Kang,^b Rongming Wang,^{a,b,*} Daofeng Sun,^{a,b,*} and Jianzhuang Jiang^{a,c,*}

a College of Science, China University of Petroleum (East China), Qingdao Shandong 266580, People's Republic of China. E-mail: rmwang@upc.edu.cn, dfsun@upc.edu.cn

b State Key Laboratory of Heavy Oil Processing, School of Materials Science and Engineering, China University of Petroleum (East China), Qingdao Shandong 266580, People's Republic of China.

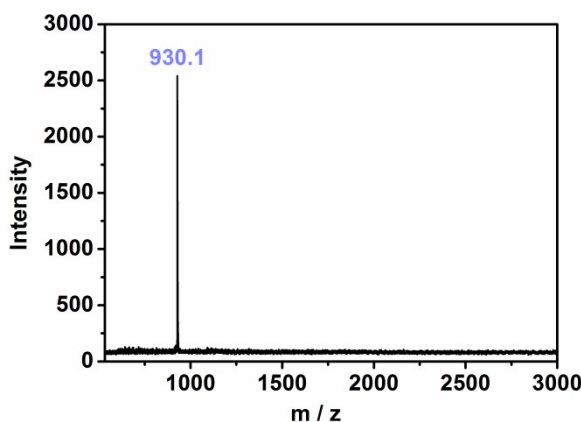
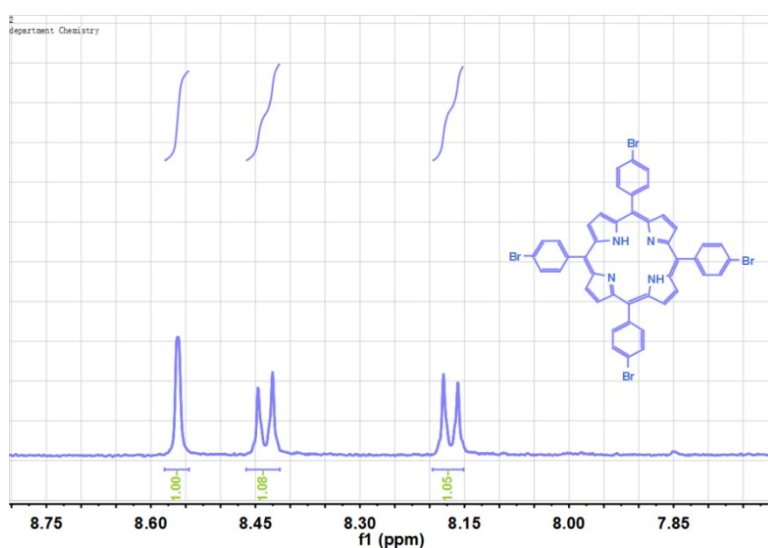
c Beijing Key Laboratory for Science and Application of Functional Molecular and Crystalline Materials, Department of Chemistry, University of Science and Technology Beijing, Beijing 100083, China. E-mail: jianzhuang@ustb.edu.cn

General synthesis methods

Key reagents including propionic acid, DMF, methanol, DCM, 1,3-diisopropylbenzene used as received from the Chemical Corporation. All reactions were carried out under an N₂ atmosphere.

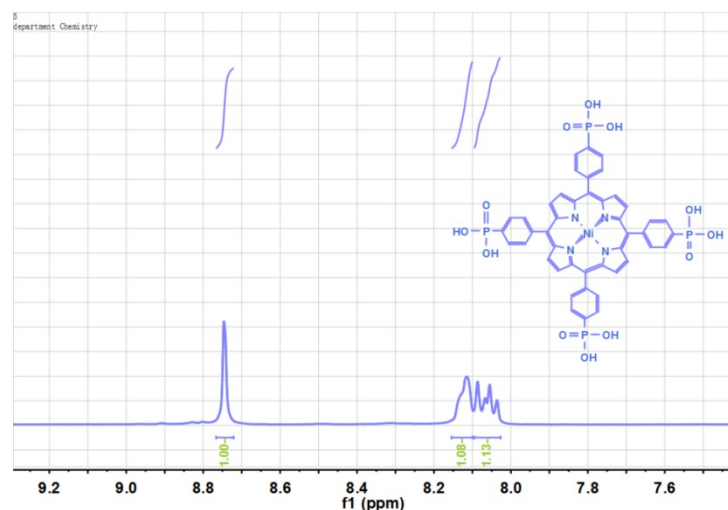
Synthesis of 5,10,15,20-tetrakis(4-bromophenyl) porphyrin (H₂TBrPP)¹

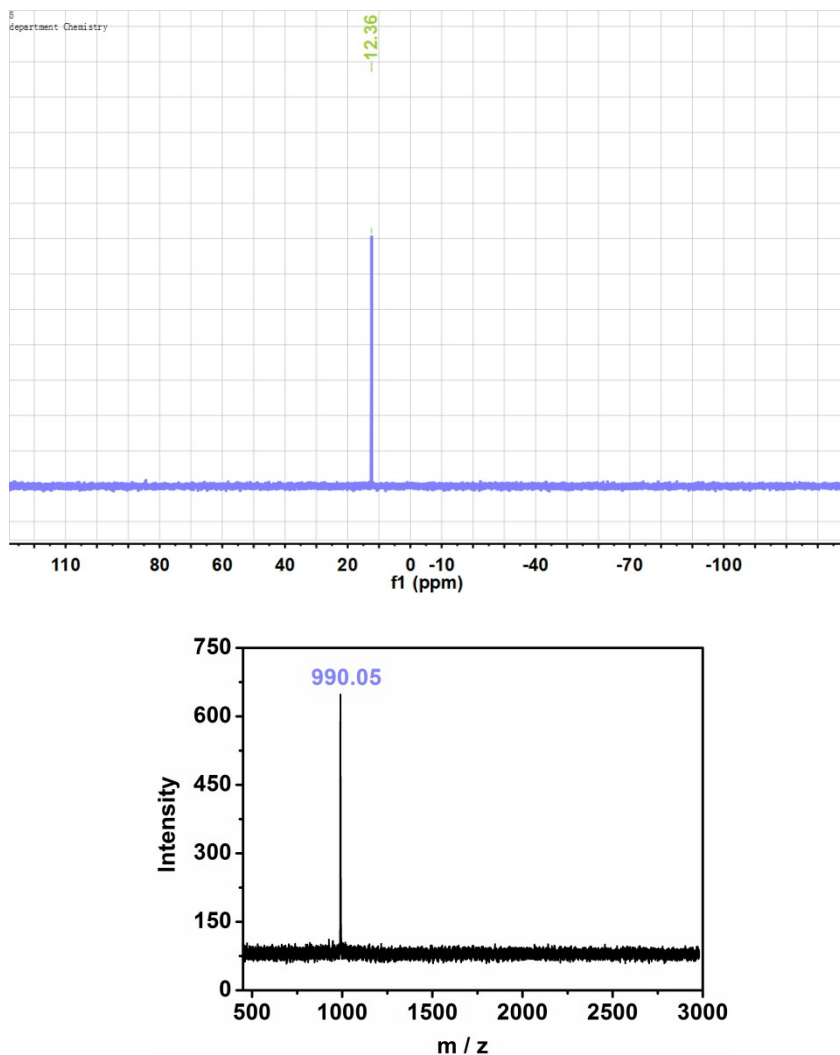
3.5 mL (0.05 mol) pyrrole and 9 g (0.05 mol) 4-bromobenzaldehyde were added to 200 mL of refluxing propionic acid. After refluxing at 141 °C for 1h, the reaction mixture was cooled to room temperature. After filtration, the solid was washed with methanol and hot water several times and purified by column chromatography on silica gel eluting by n-Hexane/dichloromethane (DCM) 1:1 system. Yield 25 %. ¹H-NMR: (400 MHz CDCl₃): δ = 8.56 (s, 8H); 8.45 (d, 8H); 8.16 (d, 8H); 7.26 (s, 1H, CDCl₃); MALDI-TOF mass spectrum: calcd for C₄₄H₂₆Br₄N₄, 929.9; found, 930.1.



Synthesis of 5,10,15,20-tetrakis(4-phosphonophenyl) porphyrin Nickel(II) (Ni-H₈TPPP)²

H₂TBrPP (3.42 g, 3.7 mmol) and anhydrous NiCl₂ (1.79 g, 13.8 mmol) were added into 70 mL 1,3-diisopropylbenzene and degassed for 30 min with N₂. The mixture was heated up to exactly 170 °C under N₂ atmosphere, then triethylphosphite (7.05 mL, 43.7 mmol) was dropped slowly to the reaction mixture in 30 min, and the reaction kept for 24 h at 170 °C. The reaction mixture was cooled down to room temperature and the resulting precipitate was filtered off and washed with 250 mL DCM. The resulting organic phase was washed 2 times each with 100 mL H₂O. The organic solvents were evaporated under reduced pressure and the resulting precipitate was hydrolyzed with 80 mL concentrated HCl at 110 °C for 72 h. The resulting product was filtered off, washed with 100 mL cooled water and afterwards stirred in 100 mL DCM for 24 h. The resulting clean product was filtered off and dried at 70 °C in a drying oven overnight. A red powder of Ni-H₈TPPP 2.74 g (2.76 mmol, 75 %) was obtained. ¹H-NMR: (400 MHz DMSO-d6): δ = 8.75 (s, 8H, H-1); 8.11 (dd, 8H, H-2); 8.06 (dd, 8H, H-3); 2.50 (s, 6H, DMSO-d6); ³¹P-NMR: (500 MHz DMSO-d6): δ = 12.36 (s, 4P, -PO(OH)₂) ppm; MALDI-TOF mass spectrum: calcd for C₄₄H₃₂N₄NiO₁₂P₄, 990.03; found, 990.05.





Synthesis of UPC-H5

Ni-H₈TPPP (1.5 mg, 0.0015 mmol) was dissolved in DMF-H₂O-CH₃COCH₃ (5:1:1, 2.1 mL) in a 10 mL vial, and reacted under solvothermal conditions for 72 h at 90 °C. The purple bulk crystals of UPC-H5 suitable for single crystal x-ray diffraction analysis were obtained with a yield of 60%. Elemental analysis calcd (%) for **UPC-H5** (C₅₅H₇₅N₉NiO₁₇P₄): C 50.16, H 5.74, N 9.57; found: C 50.01, H 5.60, N 9.39.

Synthesis of UPC-H5a

UPC-H5 was immersed in DCM with low boiling point for 24 h to conduct lattice solvent exchange. After filtration, solvent-exchanged UPC-H5 was heated to 80 °C under vacuum for 24 h to generate UPC-H5a. Elemental analysis calcd (%) for **UPC-H5a** (C₅₂H₆₀N₈NiO₁₂P₄): C 53.30, H 5.16, N 9.56; found: C 52.50, H 5.08, N 9.37.

Preparation of **UPC-H5a@NH₃·H₂O**

UPC-H5a (10 mg) was put in a 10 mL uncapped vial, then the vial was put in a 100 mL silk mouth bottle containing 10 mL 25% ammonia water and sealed. **UPC-H5a@NH₃·H₂O** were obtained by vapor diffusion at room temperature for 24 h. Elemental analysis calcd (%) for **UPC-H5a@NH₃·H₂O** ($C_{48}H_{60}N_8NiO_{16}P_4$): C 48.54, H 5.09, N 9.44; found: C 48.82, H 5.03, N 9.48.

X-ray Crystallography.

Single-crystal data of UPC-H5 was measured by an Agilent Super Nova Dual diffractometer using Cu/K α radiation ($\lambda = 1.54178 \text{ \AA}$) at 150 K and focusing multilayer mirror optics. The structures were solved by direct methods using SHELXTL and refined by full-matrix least squares on F² using SHELX-97. All non-hydrogen atoms were refined with anisotropic displacement parameters during the final cycles. The crystallographic collection and refinement parameters are listed in Table S1. The crystallographic data was deposited in the Cambridge Crystallographic Data Center (CCDC 1976307 for UPC-H5). These data can be obtained free of charge from the CCDC via www.ccdc.cam.ac.uk.

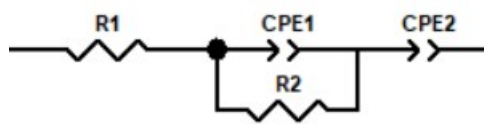
The water vapor adsorption tests.

The water vapor adsorption and desorption curves were measured by IGA-100B intelligent gravimetric analyzer of (Hiden) Company of Hyde Company, UK. The tests of three HOFs were conducted after removing the lattice water molecules and free water molecules that may be adsorbed in air. Meanwhile, the water adsorption isotherms of **UPC-H5** and **UPC-H5a** were recorded after vacuuming the sample for 5 hours at 298 K, but the test of **UPC-H5a@NH₃·H₂O** was performed after heating the sample for 5 hours at 378 K under vacuum. At every humidity point, the samples were stabled for 2-3 hours to reach adsorption equilibrium.

Measurements of proton conductivity.

The pelletized samples for proton conductivity were prepared by the following procedures: The as-synthesized sample (**UPC-H5**, **UPC-H5a** and **UPC-H5a@NH₃·H₂O**) was placed in a 2.98 mm diameter mold and pressed into a pellet at 1 MPa for 1 min with a diameter of 2.98 mm and a thickness in the range of 0.5-1 mm by a tabletting machine. The pelletized sample was placed in

the center of the glass plate and fixed horizontally with two 20 cm of gold wires, and two sides of pelletized sample were coated with silver glue, and then waited for about 30 minutes to dry. Impedance analysis was performed with a 1260A Impedance/Gain-Phase Analyzer from 10 MHz to 0.1 Hz with an input voltage 200 mV in a constant temperature and humidity. Humidity and temperature were controlled by using a BPS-50CL humidity control chamber. The impedance values at each temperature were repeatedly measured after 30 minutes of equilibrium until the measured values keep no change. The resistance values was obtained by fitting the impedance profile using zview software. The circuit equivalent used for fitting is as follows:



R_1 corresponds to the resistances of wire and electrode, while R_2 accounts for the bulk resistance of the pellet. CPE1 and CPE2 denote the nonideal capacitance corresponding to the bulk and non-ideal capacitance for grain boundary.

Proton conductivity was calculated using the following equation:

$$\sigma = \frac{l}{RS}$$

l and S are the thickness (cm) and cross-sectional area (cm^2) of the pellet, respectively. R is the bulk resistance of the pellet (R_2 in the circuit equivalent) fitted by the equivalent circuit of the semicircle in Nyquist plot using zview software. The activation energy (E_a) of the material conductivity is estimated according to the following equation:

$$\sigma T = \sigma_0 \exp\left(-\frac{E_a}{k_B T}\right)$$

where σ is the proton conductivity, σ_0 is the pre-exponential factor, k_B is the Boltzmann constant, and T is the temperature.

Other measurements.

The $^1\text{H-NMR}$ spectra were recorded on a Bruker DRX 500 spectrometer. MALDI-TOF mass spectrometry was performed on a Bruker BIFLEX III with ultra-high resolution. The date of powder X-ray diffraction (PXRD) were recorded on an X-Pert PRO MPD diffractometer with $\text{Cu-K}\alpha$ radiation ($\lambda = 0.154178 \text{ nm}$). Thermal gravimetric analysis (TGA) was proceeded on a Mettler Toledo TGA instrument in the range of 40-900 °C with a heating rate of 10 °C min^{-1} under N_2 .

atmosphere (100 mL min⁻¹). Elemental analysis was conducted on a PerkinElmer 240C elemental analyzer for C, H, and N determination. N₂ and CO₂ adsorption and desorption tests were performed on a Micromeritics ASAP 2020 surface area analyzer. Infrared (IR) spectra were obtained on a Nicolet 330 FTIR spectrometer. X-ray photoelectron spectroscopy (XPS) was conducted on VG ESCALAB 220i-XL equipped with Al K α X-ray source.

Table S1. Crystallographic and Refinement Parameters for **UPC-H5**

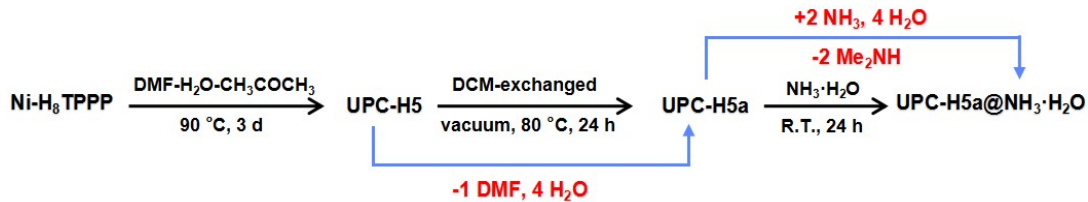
Crystal data	UPC-H5
System	Triclinic
Space group	<i>P</i> \bar{I}
MF	C ₅₅ H ₇₅ N ₉ NiO ₁₇ P ₄
FW	1316.82
a/ \AA	10.4362(4)
b/ \AA	15.4540(5)
c/ \AA	19.9620(8)
$\alpha/^\circ$	82.370(3)
$\beta/^\circ$	79.379(3)
$\gamma/^\circ$	84.353(3)
Volume/ \AA^3	3127.3(2)
Z	2
Density/g $\cdot\text{cm}^3$	1.398
μ/mm^{-1}	2.046
F(000)	1384.0
R_1^a I>2 θ	0.0701
R_{w2}^b I>2 θ	0.1897
R_1^a	0.0985
R_{w2}^b	0.2156
CCDC no.	1976307

^a $R_1 = \sum |F_O - |F_C|| / \sum |F_O|$, ^b $R_{w2} = [\sum w(F_O^2 - F_C^2)^2 / \sum w(F_O^2)]^{1/2}$.

Table S2. Hydrogen Bonded parameters in **UPC-H5**

D-H···A	Distance of H···A (Å)	Distance of D···A (Å)	Angle of D-H···A (°)
O3-H3···O11 ^{#1}	1.65	2.54	170.0
O5-H5···O7 ^{#5}	1.67	2.56	166.2
O8-H8···O4 ^{#2}	1.57	2.47	174.6
O10-H10···O9 ^{#8}	1.71	2.59	166.3
N5-H5B···O12 ^{#1}	1.84	2.73	171.0
N5-H5C···O6	1.86	2.75	167.0
N6-H6A···O1 ^{#10}	1.77	2.67	172.4
N6-H6B···O9	1.82	2.71	167.1
N7-H7A···O6 ^{#8}	1.84	2.72	165.1
N7-H7B···O2	1.76	2.66	177.8
N8B-H8B···O7 ^{#9}	1.90	2.73	153.1
N8-H8C···O1W ^{#8}	1.85	2.72	162.1
O1W-H1WA···O12 ^{#3}	2.01	2.86	178.6
O1W-H1WB···O2 ^{#4}	1.89	2.73	166.7
O2W-H2WA···O1	2.02	2.87	166.8
O2W-H2WB···O11 ^{#1}	2.10	2.79	137.0
O3W-H3WA···O2W ^{#1}	1.98	2.78	155.8
O3W-H3WB···O1 ^{#4}	1.96	2.83	174.2
O14-H14A···O3W ^{#1}	2.33	3.00	136.0

^a Symmetric code, #1: 1-x, -y, 1-z, #2: 1+x, -1+y, z, #3: x, -1+y, z, #4: -1+x, y, z, #5: -1+x, -1+y, z, #6: 2-x, -y, -z, #7: 2-x, -1-y, 1-z, #8: 1-x, -y, -z, #9: x, 1+y, z, #10: 2-x, -y, 1-z.



Scheme S1. Synthetic and guest-tuned route for **UPC-H5**, **UPC-H5a** and **UPC-H5a@NH₃·H₂O**.

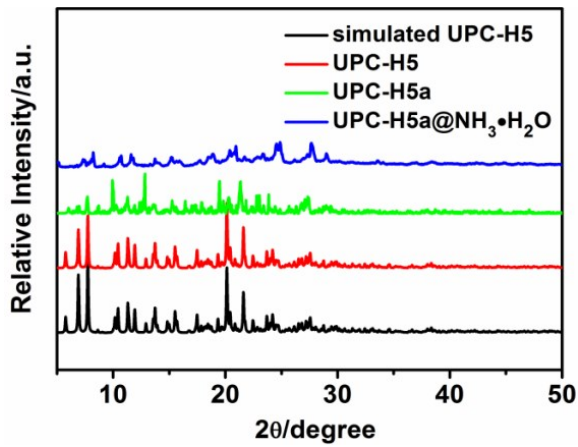


Fig. S1 PXRD patterns of **UPC-H5**, **UPC-H5a** and **UPC-H5a@NH₃·H₂O**.

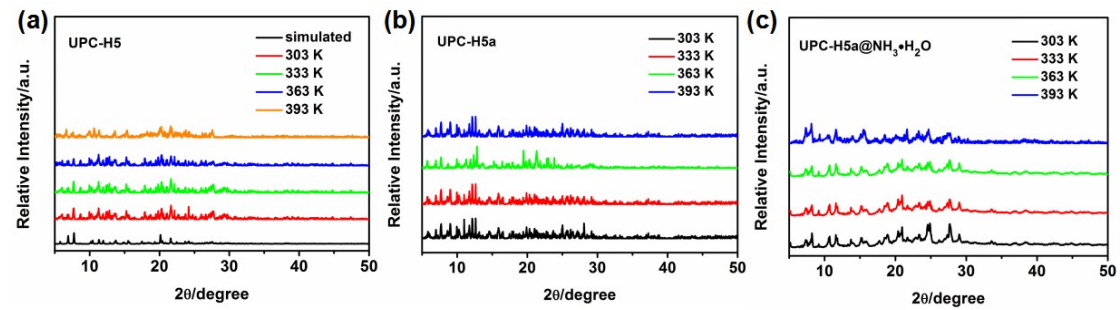


Fig. S2 In-situ PXRD patterns: (a) **UPC-H5**, (b) **UPC-H5a** and (c) **UPC-H5a@NH₃·H₂O**.

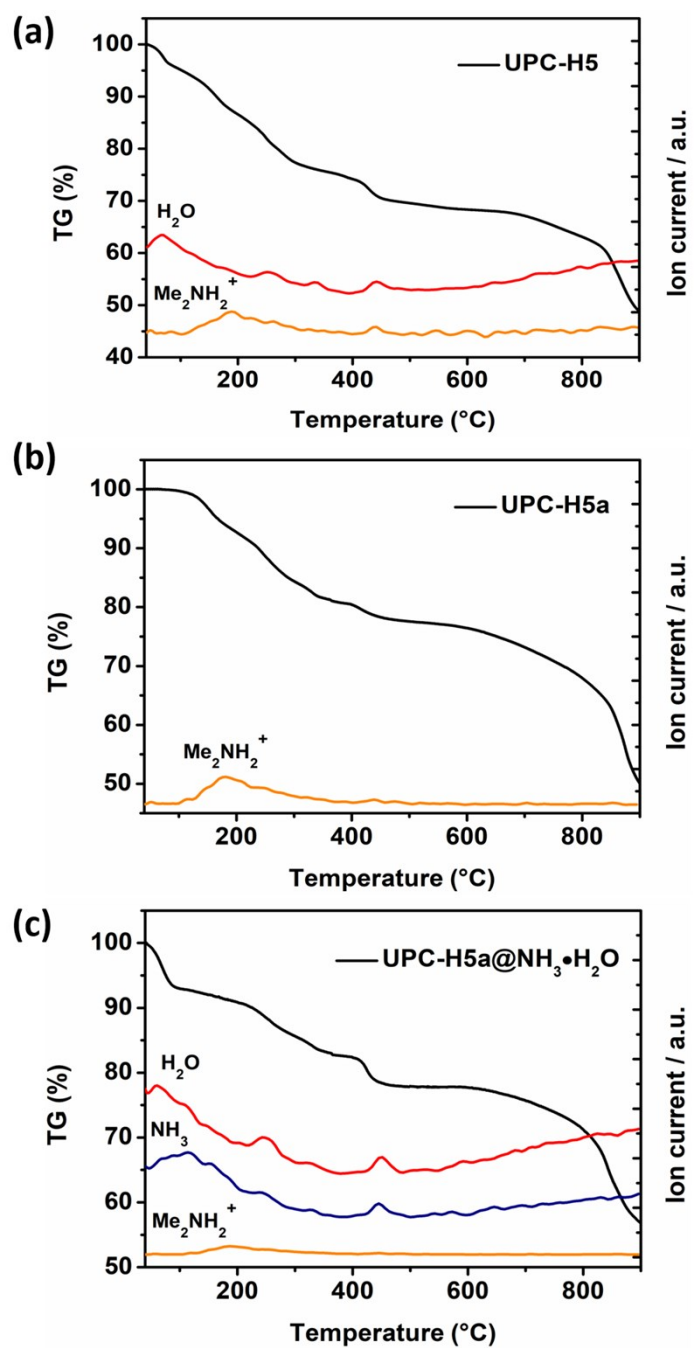


Fig. S3 TG-MS curves of **UPC-H5** (a), **UPC-H5a** (b) and **UPC-H5a@NH₃·H₂O** (c) in the range of 40-900 °C with the heating rate of 10 °C min⁻¹ under He.

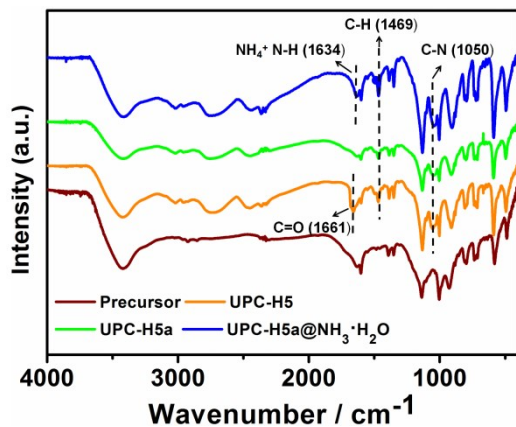


Fig. S4 Infrared spectra of precursor (NiH₄TPPP), **UPC-H5**, **UPC-H5a** and **UPC-H5a@NH₃·H₂O**.

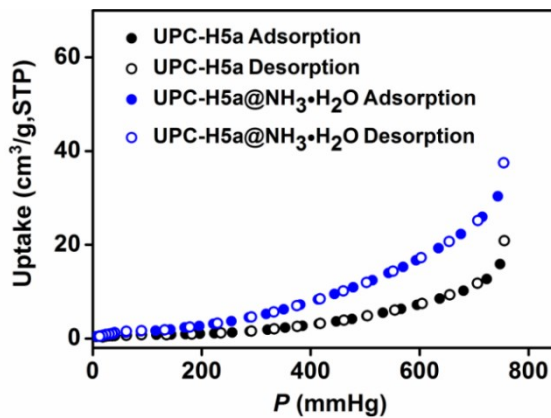


Fig. S5 N₂ adsorption/desorption isotherms of **UPC-H5a** and **UPC-H5a@NH₃·H₂O** at 77 k.

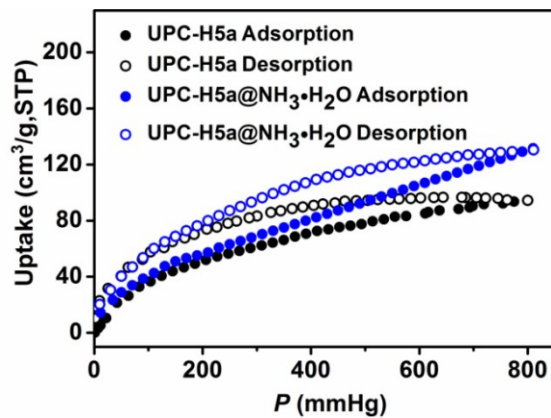


Fig. S6 CO₂ adsorption/desorption isotherms of **UPC-H5a** and **UPC-H5a@NH₃·H₂O** at 196 k.

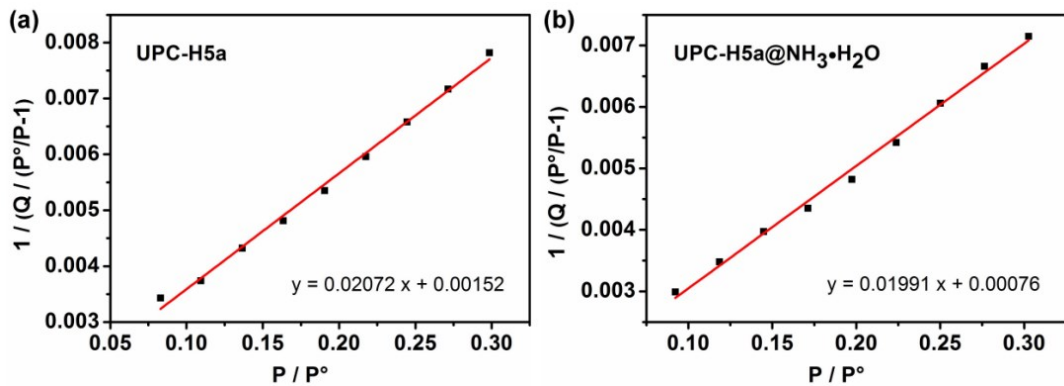


Fig. S7 (a) The BET surface area of **UPC-H5a** obtained from the CO₂ adsorption isotherm at 196 K. SBET = $(1/(0.02072-0.00152))/22414 \times 6.023 \times 10^{23} \times 0.170 \times 10^{-18} = 237.5 \text{ m}^2 \text{ g}^{-1}$; (b) The BET surface area of **UPC-H5a@NH₃·H₂O** obtained from the CO₂ adsorption isotherm at 196 K. SBET = $(1/(0.01991-0.00076))/22414 \times 6.023 \times 10^{23} \times 0.170 \times 10^{-18} = 371.1 \text{ m}^2 \text{ g}^{-1}$.

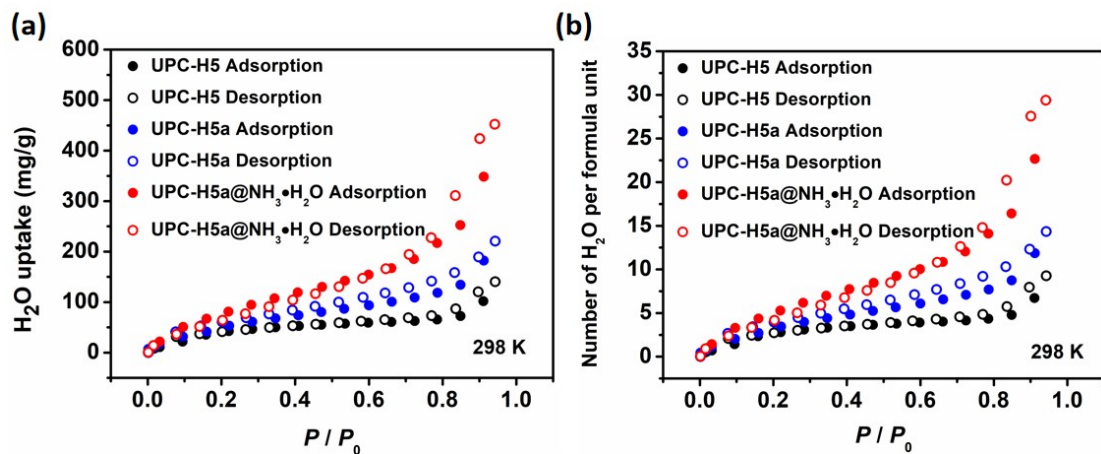


Fig. S8 Water adsorption isotherms of **UPC-H5**, **UPC-H5a** and **UPC-H5a@NH₃·H₂O** at 298 K.

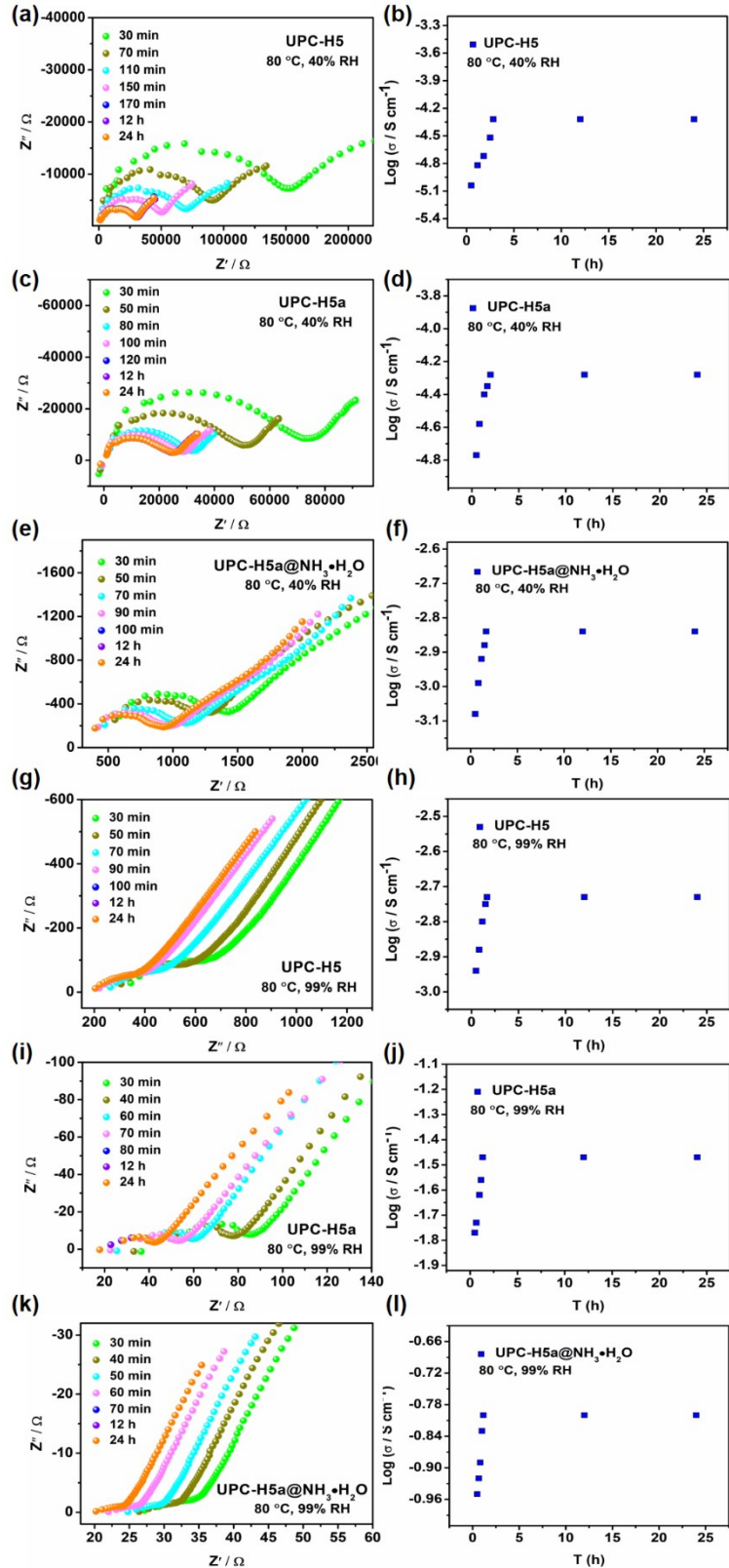


Fig. S9 The time-dependent Nyquist plots of **UPC-H5** (a), **UPC-H5a** (c) and **UPC-H5a@NH₃·H₂O** (e) and time-dependent proton conductivity of **UPC-H5**, **UPC-H5a** (d) and **UPC-H5a@NH₃·H₂O** (f) at $80\text{ }^{\circ}\text{C}$, 40% R.H.; the time-dependent Nyquist plots of **UPC-H5** (g), **UPC-H5a** (i) and **UPC-H5a@NH₃·H₂O** (k) and time-dependent proton conductivity of **UPC-H5** (h), **UPC-H5a** (j) and **UPC-H5a@NH₃·H₂O** (l) at $80\text{ }^{\circ}\text{C}$, 99% R.H.

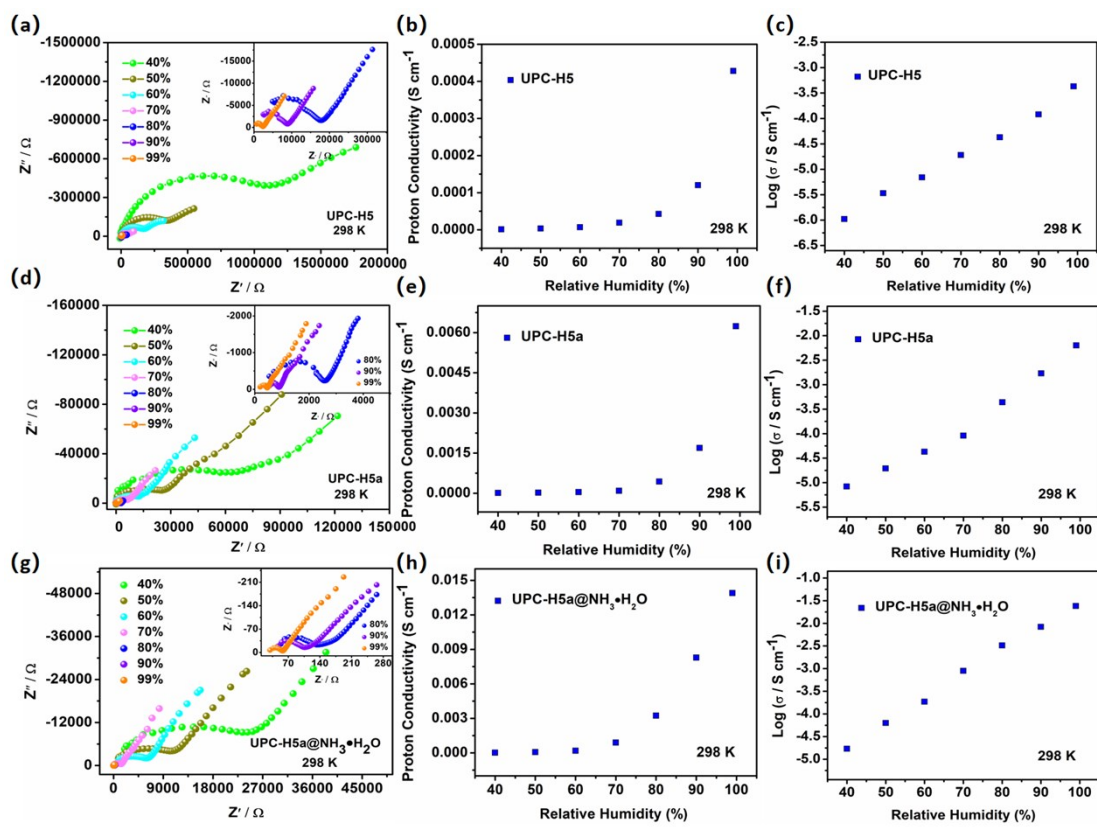


Fig. S10 Nyquist plots of **UPC-H5** (a), **UPC-H5a** (d) and **UPC-H5a@NH₃·H₂O** (g) at 298 K under different R.H.; and humidity-dependent proton conductivity of **UPC-H5** (b) (c), **UPC-H5a** (e) (f) and **UPC-H5a@NH₃·H₂O** (h) (i).

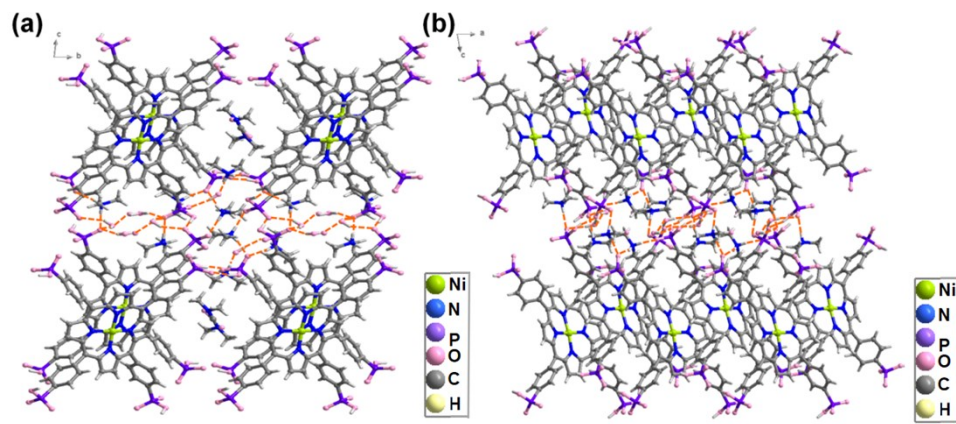


Fig. S11 Hydrogen-bonding network of **UPC-H5** showing the proton transfer pathways viewed along **a** axis (a) and along **b** axis (b).

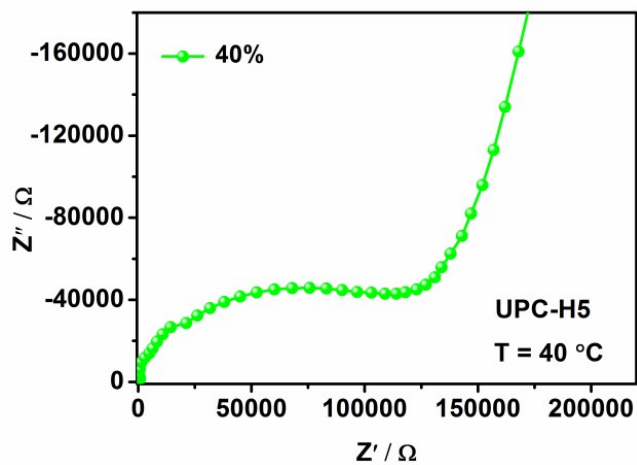


Fig. S12 Nyquist plot of **UPC-H5** at 40 °C and under 40% RH.

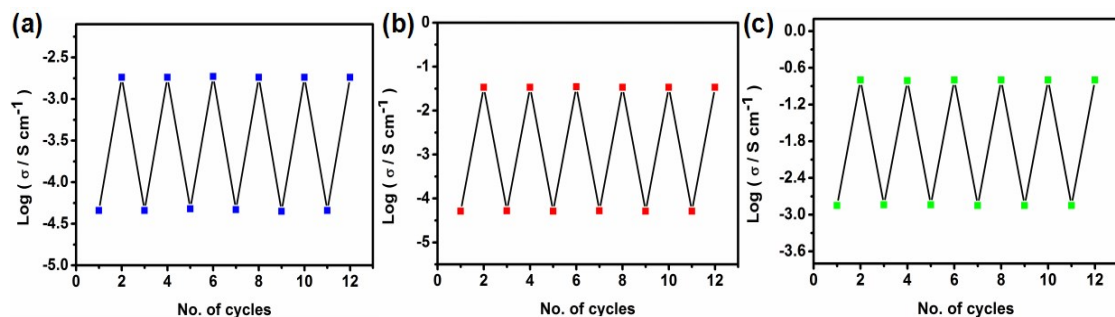


Fig. S13 Cycling tests of **UPC-H5** (a), **UPC-H5a** (b) and **UPC-H5a@NH₃·H₂O** (c) between 40% RH and 99% R.H. at 80 °C.

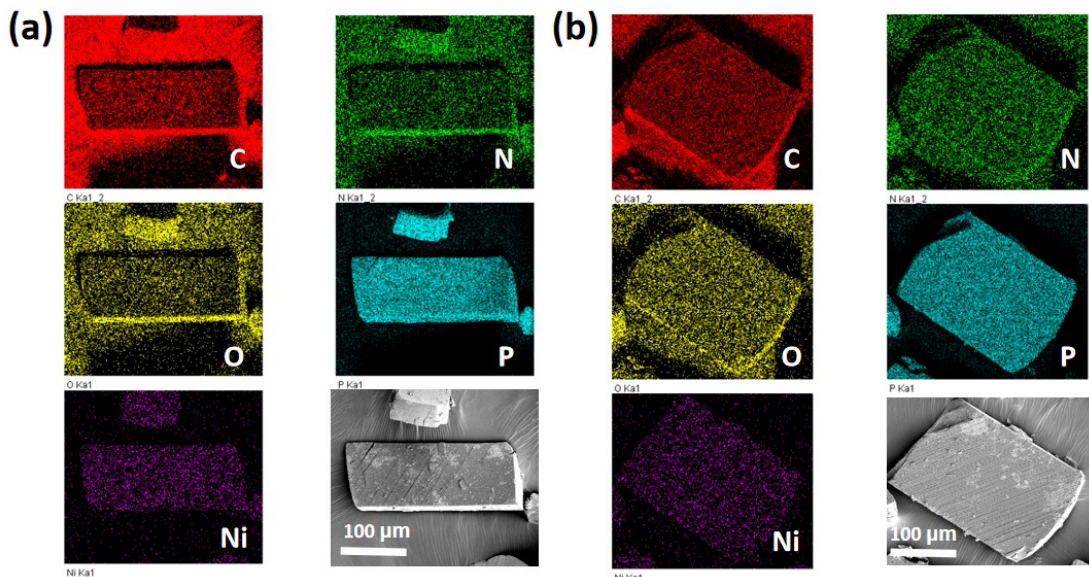


Fig. S14 EDS elemental mapping images of C Ka_1 , N Ka_1 , O Ka_1 , P Ka_1 , Ni Ka_1 for **UPC-H5a@NH₃·H₂O** before (a) and after (b) placing one week at 80 °C and 99% R.H..

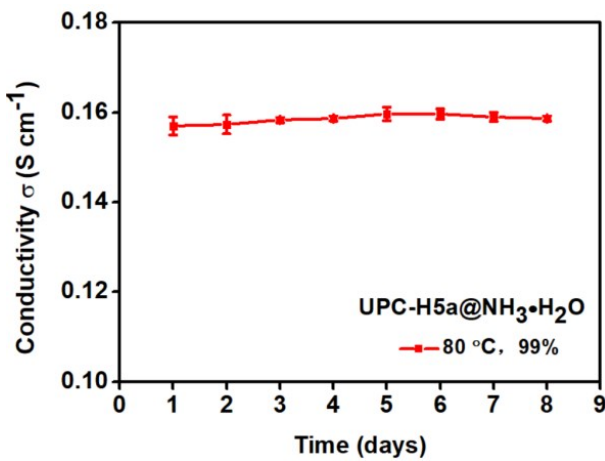


Fig. S15 Stability tests of UPC-H5a@NH₃·H₂O at 80 °C and 99% R.H. for one week.

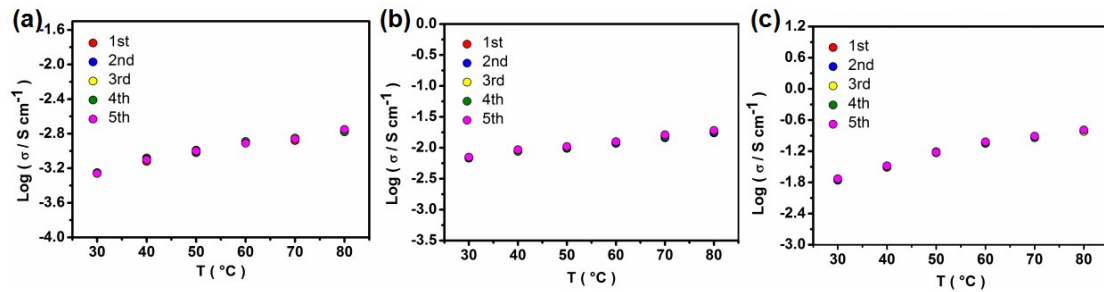


Fig. S16 Cycling tests of the temperature-dependent conductivity of **UPC-H5** (a), **UPC-H5a** (b) and **UPC-H5a@NH₃·H₂O** (c) at 95 % R.H.

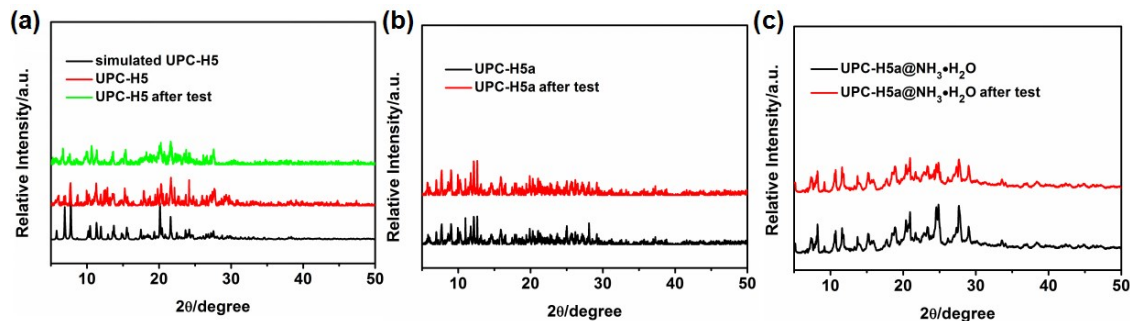


Fig. S17 PXRD patterns of **UPC-H5**, **UPC-H5a** and **UPC-H5a@NH₃·H₂O** before and after temperature-dependent and humidity-dependent impedance tests.

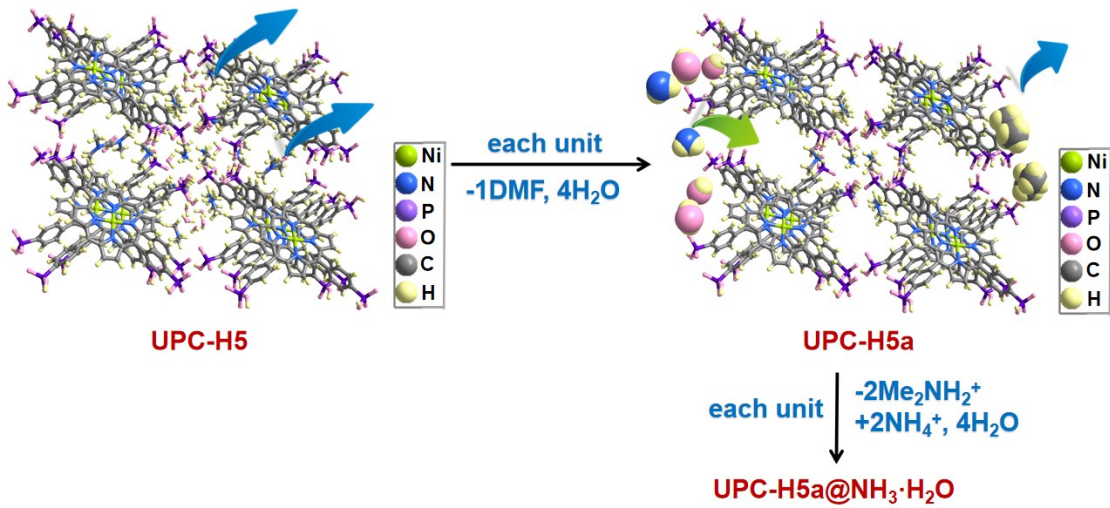


Fig. S18 The guest change in the two-step tuned process viewed along a axis. Note: the structure of UPC-H5a is illustrated using the crystal data of **UPC-H5** owing to their slight change of structure as indicated by PXRD tests.

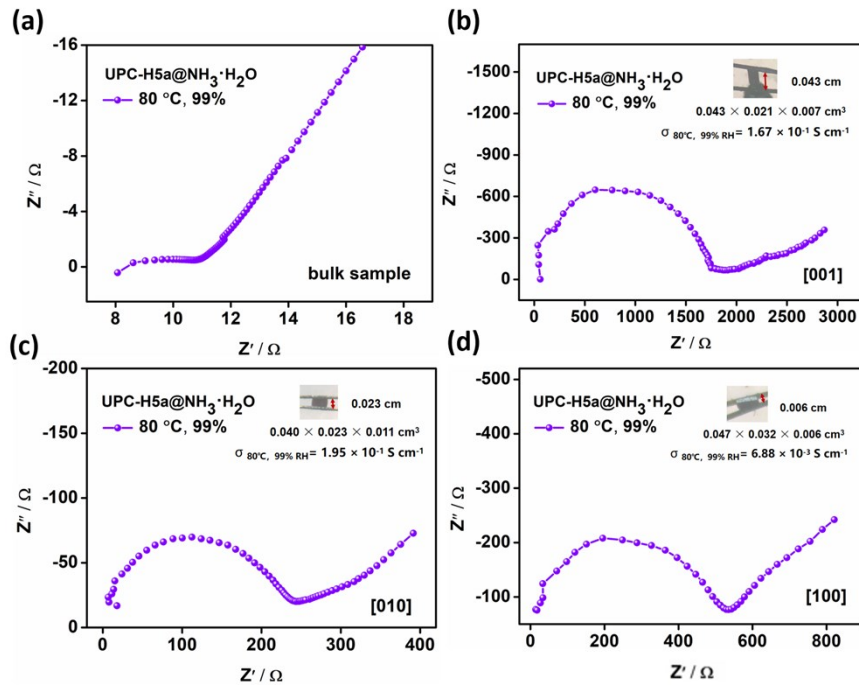


Fig. S19 Nyquist plots of pellet (a) and single crystal (b-d) of **UPC-H5a@NH₃·H₂O** at 80 °C and 99% R.H. (inset: Au wires are glued with a crystal of **UPC-H5a@NH₃·H₂O** along [001], [010] and [100]). Note: the [001] direction is viewed according to the single crystal of UPC-H5 because the crystals of UPC-H5 and UPC-H5a@NH₃·H₂O have the same shape.

Table S3. Humidity-dependent proton conductivities of three HOFs at 25 °C.

Conditions	Conductivity of UPC-H5 (S cm ⁻¹)	Conductivity of UPC-H5a (S cm ⁻¹)	Conductivity of UPC-H5a@NH ₃ .H ₂ O (S cm ⁻¹)
25 °C, 40 % R. H.	1.04×10^{-6}	8.23×10^{-6}	1.68×10^{-5}
25 °C, 50 % R. H.	3.36×10^{-6}	1.94×10^{-5}	6.28×10^{-5}
25 °C, 60 % R. H.	6.90×10^{-6}	4.28×10^{-5}	1.87×10^{-4}
25 °C, 70 % R. H.	1.89×10^{-5}	9.03×10^{-5}	8.94×10^{-4}
25 °C, 80 % R. H.	4.27×10^{-5}	4.36×10^{-4}	3.23×10^{-3}
25 °C, 90 % R. H.	1.21×10^{-4}	1.69×10^{-3}	8.28×10^{-3}
25 °C, 99 % R. H.	4.28×10^{-4}	6.24×10^{-3}	1.39×10^{-2}

Table S4. Humidity-dependent proton conductivities of three HOFs at 80 °C.

Conditions	Conductivity of UPC-H5 (S cm ⁻¹)	Conductivity of UPC-H5a (S cm ⁻¹)	Conductivity of UPC-H5a@NH ₃ .H ₂ O (S cm ⁻¹)
80 °C, 40 % R. H.	4.68×10^{-5}	5.22×10^{-5}	1.43×10^{-3}
80 °C, 50 % R. H.	8.72×10^{-5}	1.28×10^{-4}	2.49×10^{-3}
80 °C, 60 % R. H.	2.13×10^{-4}	3.84×10^{-4}	3.77×10^{-3}
80 °C, 70 % R. H.	4.43×10^{-4}	8.28×10^{-4}	8.34×10^{-3}
80 °C, 80 % R. H.	7.97×10^{-4}	2.14×10^{-3}	1.50×10^{-2}
80 °C, 90 % R. H.	1.33×10^{-3}	7.70×10^{-3}	5.05×10^{-2}
80 °C, 95 % R. H.	1.67×10^{-3}	1.70×10^{-2}	7.43×10^{-2}
80 °C, 99 % R. H.	1.85×10^{-3}	3.42×10^{-2}	1.59×10^{-1}

Table S5. Comparison of proton conductivity of UPC-H5a@NH₃·H₂O with the reported materials up to 10⁻² S cm⁻¹.

Compounds	Conductivity y (S cm ⁻¹)	Conditions	E _a (eV)	References
[Gd ₂ (H ₃ nmp) ₂]·xH ₂ O	5.10 × 10 ⁻¹	94 °C, 98 % R. H.	-	3
NC3-5 (Nafion-Cage)	2.70 × 10 ⁻¹	90 °C, 95 % R. H.	-	4
PSS@ZIF-8	2.59 × 10 ⁻¹	80 °C, 100 % R. H.	0.543	5
PSM 1 (UiO-66-based)	1.64 × 10 ⁻¹	80 °C, 95 % R. H.	0.11	6
Cr-MIL-88B-PESA	1.58 × 10 ⁻¹	100 °C, 85 % R. H.	0.40	7
UPC-H5a@NH₃·H₂O	1.57 × 10⁻¹	80 °C, 99 % R. H.	0.40	This work
IM-UiO-66-AS	1.54 × 10 ⁻¹	80 °C, 98 % R. H.	0.32	8
Co-tri	1.49 × 10 ⁻¹	80 °C, 98 % R. H.	0.40	9
H ₂ SO ₄ (1M)@MIL-101(Cr)-NH-(CH ₂) ₃ SO ₃ H	1.31 × 10 ⁻¹	90 °C, 95 % R. H.	0.17	10
C-SPAEKS/Im-MOF-801-4%	1.28 × 10 ⁻¹	90 °C, 100 % R. H.	-	11
BUT-8-(Cr)A	1.27 × 10 ⁻¹	80 °C, 100 % R. H.	0.11	12
PCMOF2½(Tz)	1.17 × 10 ⁻¹	85 °C, 90 % R. H.	0.12	13
FCF-1	1.17 × 10 ⁻¹	100 °C, 98 % R. H.	0.60	14
H ₃ PO ₄ @NKCOF-1	1.13 × 10 ⁻¹	80 °C, 98 % R. H.	0.14	15
PCMOF2½(Pz)	1.10 × 10 ⁻¹	85 °C, 90 % R. H.	0.16	13
CBA/Nafion-PVA	1.10 × 10 ⁻¹	80 °C, 98 % R. H.	-	16
H ₃ PO ₄ @HUP-2	1.02 × 10 ⁻¹	98 °C, 98 % R. H.	0.10	17
Nafion (sulfonated polymer)	1.00 × 10 ⁻¹	80 °C, 100 % R. H.	0.22	18
MOF UiO-66(SO ₃ H) ₂	8.4 × 10 ⁻²	80 °C, 90 % R. H.	0.32	19
TfOH@MIL-101	8.2 × 10 ⁻²	60 °C, 15 % R. H.	0.18	20
PTSA@TpAzo COFM	7.8 × 10 ⁻²	80 °C, 95 % R. H.	0.16	21
CPM-103a -single crystal	5.8 × 10 ⁻²	22.5 °C, 98 % R. H.	0.66	22
TJU-102	5.26 × 10 ⁻²	90 °C, 98 % R. H.	0.59	23
(NH ₃ (CH ₂) ₃ NH ₃) ₂ -	5.00 × 10 ⁻²	40 °C, NH ₃	0.32	24
[Fe ₄ (OH) ₃ (HPO ₄) ₂ (PO ₄) ₃]·4H ₂ O				
HImMo132	4.98 × 10 ⁻²	90 °C, 98 % R. H.	0.51	25
Co-tetra	4.15 × 10 ⁻²	80 °C, 98 % R. H.	0.29	9
PCMOF-10	3.55 × 10 ⁻²	70 °C, 95 % R. H.	0.40	26
COF BIP	3.55 × 10 ⁻²	95 °C, 95 % R. H.	0.31	27
Im@MOF-808	3.45 × 10 ⁻²	65 °C, 99 % R. H.	0.25	28
MPOPS-1	3.07 × 10 ⁻²	77 °C, 95 % R. H.	0.41	29
MIP-177-SO ₄ H-LT	2.60 × 10 ⁻²	25 °C, 95 % R. H.	-	30
{[Tb ₄ (TTHA) ₂ (H ₂ O) ₄]·7H ₂ O} _n	2.57 × 10 ⁻²	60 °C, 98 % R. H.	0.68	31
CPOS-2	2.2 × 10 ⁻²	60 °C, 99 % R. H.	-	32
[NiV ₂ O ₆ H ₈ (P ₂ O ₇) ₂]·2H ₂ O	2.00 × 10 ⁻²	60 °C, 98 % R. H.	0.38	33
HOF-GS-11	1.80 × 10 ⁻²	30 °C, 95 % R. H.	0.135	34
P ₂ Mo ₅ -EN	1.13 × 10 ⁻²	65 °C, 95 % R. H.	0.4	35

FCF-2	1.10×10^{-2}	100 °C, 98 % R. H.	0.23	14
MIP-202(Zr)	1.10×10^{-2}	90 °C, 95 % R. H.	0.22	36
CPOS-1	1.0×10^{-2}	60 °C, 99 % R. H.	-	32
HOF-GS-10	0.75×10^{-2}	30 °C, 95 % R. H.	0.489	34

References:

- [1] V. Mamane, I. Ledoux-Rak, S. Deveau, J. Zyss, O. Riant, *Synthesis* 2003, **3**, 455-467.
- [2] T. Rhuderwiek, K. Wolkersdorfer, S. Øien-Ødegaard, K. P. Lillerud, M. Wark, N. Stock, *Chem. Commun.* 2018, **54**, 389-392.
- [3] R. F. Mendes, P. Barbosa, E. M. Domingues, P. Silva, F. Figueiredo, F. A. A. Paz, *Chem. Sci.*, 2020, **11**, 6305–6311.
- [4] R. Han, P. Wu, *ACS Appl. Mater. Interfaces* 2018, **10**, 18351-18358.
- [5] Y. Cai, Q. Yang, Z. Zhu, Q. Sun, A. Zhu, Q. Zhang, Q. Liu, *J. Membrane. Sci* 2019, **590**, 117277.
- [6] H. Sun, B. Tang, P. Wu, *ACS Appl. Mater. Interfaces* 2019, **11**, 13423-13432.
- [7] S. Liu, Z. Han, J. Yang, S. Huang, X. Dong, S. Zang, *Inorganic Chemistry* 2020, **59**, 1, 396.
- [8] X. Li, J. Liu, C. Zhao, J. Zhou, L. Zhao, S. Li, Y. Lan, *J. Mater. Chem. A*, 2019, **7**, 25165.
- [9] S. M. Elahi, S. Chand, W. H. Deng, A. Pal, M. C. Das, *Angew. Chem. Int. Ed.* 2018, **57**, 6662-6666.
- [10] S. Devautour-Viont, E. S. Sanil, A. Genest, V. Ortiz, P. G. Yot, J. Chang, G. Maurin, *Chem. Asian J.*, 2019, **14**, 3561.
- [11] Z. Zhang, J. Ren, J. Xu, Z. Wang, W. He, S. Wang, X. Yang, X. Du, L. Meng, P. Zhao, *J. Membrane. Sci* 2020, 607, 118194.
- [12] F. Yang, G. Xu, Y. Dou, B. Wang, H. Zhang, H. Wu, W. Zhou, J. R. Li, B. Chen, *Nat. Energy* 2017, **2**, 877-883.
- [13] S. Kim, B. Joarder, J. A. Hurd, J. Zhang, K. W. Dawson, B. S. Gelfand, N. E. Wong, G. K. H. Shimizu, *J. Am. Chem. Soc.* 2018, **140**, 1077-1082.
- [14] Y. Qin, T. Gao, W. Xie, Z. Li, G. Li, *ACS Appl. Mater. Interfaces* 2019, **11**, 31018-31027.
- [15] Y. Yang, P. Cheng, Z. Zhang, *Angew. Chem. Int. Ed.* 2020, **59**, 2-9.
- [16] Y. Li, L. Liang, C. Liu, Y. Li, W. Xing, J. Sun, *Adv. Mater.* 2018, **30**, 1707146.
- [17] D. Gui, W. Duan, J. Shu, F. Zhai, N. Wang, X. Wang, J. Xie, H. Li, L. Chen, J. Wu, Z. Chai, S. Wang, *CCS Chem.* 2019, **1**, 197.

- [18] X. Wu, X. Wang, G. He, J. Benziger, *J. Polym. Sci., Part B: Polym. Phys.* 2011, **49**, 1437-1445.
- [19] W. J. Phang, H. Jo, W. R. Lee, J. H. Song, K. Yoo, B. Kim, C. S. Hong, *Angew. Chem. Int. Ed.* 2015, **54**, 5142-5146.
- [20] D. N. Dybtsev, V. G. Ponomareva, S. B. Aliev, A. P. Chupakhin, M. R. Gallyamov, N. K. Moroz, B. A. Kolesov, K. A. Kovalenko, E. S. Shutova, V. P. Fedin, *ACS Appl. Mater. Interfaces* 2014, **6**, 5161-5167.
- [21] H. S. Saamal, H. B. Aiyappa, S. N. Bhange, S. Karak, A. Halder, S. Kurungot, R. Banerjee, *Angew. Chem. Int. Ed.* 2018, **130**, 11060-11064.
- [22] Q. Zhai, C. Mao, X. Zhao, Q. Lin, F. Bu, X. Chen, X. Bu, P. Feng, *Angew. Chem. Int. Ed.* 2015, **54**, 7886-7890.
- [23] Y. Tian, G. Liang, T. Fan, J. Shang, S. Shang, Y. Ma, R. Matsuda, M. Liu, M. Wang, L. Li, S. Kitagawa, *Chem. Mater.* 2019, **31**, 8494-8503.
- [24] H. Zhao, Y. Jia, Y. Gu, F. He, K. Zhang, Z. Tian, J. Liu, *RSC Adv.* 2020, **10**, 9046
- [25] W. Liu, L. Dong, R. Li, Y. Chen, S. Sun, S. Li, Y. Lan, *ACS Appl. Mater. Interfaces* 2019, **11**, 7030-7036.
- [26] P. Ramaswamy, N. E. Wong, B. S. Gelfand, G. K. H. Shimizu, *J. Am. Chem. Soc.* 2015, **137**, 7640-7643.
- [27] C. R. Kayaramkodath, I. Rajith, D. Sairam, P. Joseph, C. W. Vivek, K. V. Raj, K. Sreekumar, S. B. Sukumaran, *J. Am. Chem. Soc.* 2019, **141**, 14950-14954.
- [28] H. Luo, Q. Ren, P. Wang, J. Zhang, L. Wang, X. Ren, *ACS Appl. Mater. Interfaces* 2019, **11**, 9164-9171.
- [29] P. Bhanja, A. Palui, S. Chatterjee, Y. Kaneti, J. Na, Y. Sugahara, A. Bhaumik, Y. Yamauchi, *ACS Sustainable Chem. Eng.* 2020, **8**, 2423.
- [30] M. Wahiduzzaman, S. Wang, J. Schnee, A. Vimont, V. Ortiz, P. Yot, R. Retoux, M. Daturi, J. Lee, J. Chang, C. Serre, G. Maurin, S. Devautour-Vinot, *ACS Sustainable Chem. Eng.* 2019, **7**, 5776.
- [31] L. Feng, H. Wang, H. Xu, W. Huang, T. Zeng, Q. Cheng, Z. Pan, H. Zhou, *Chem. Commun.*, 2019, **55**, 1762-1765
- [32] G. Xing, T. Yan, S. Das, T. Ben, S. Qiu, *Angew. Chem. Int. Ed.* 2018, **57**, 5345-5349.

- [33] L. Zhang, X. Liu, X. Sun, J. Jian, G. Li, H. Yuan, *Inorg. Chem.* 2019, **58**, 7, 4394.
- [34] A. Karmakar, R. Illathvalappil, B. Anothumakkool, A. Sen, P. Samanta, A. V. Desai, S. Kurungot, S. K. Ghosh, *Angew. Chem. Int. Ed.* 2016, **55**, 1-6.
- [35] S. Zhang, Y. Lu, X. Sun, Z. Li, T. Dang, S. Liu, *Dalton Trans.*, 2020, **49**, 17301-17309.
- [36] S. Wang, M. Wahiduzzaman, L. Davis, A. Tissot, W. Shepard, J. Marrot, C. Martineau-Corcos, D. Hamdane, G. Maurin, S. Devautour-Vinot, C. Serre, *Nature Communication*, 2018, **9**, 4937.

Table S6. Temperature-dependent proton conductivities of three HOFs.

Conditions	Conductivity of UPC-H5 (S cm ⁻¹)	Conductivity of UPC-H5a (S cm ⁻¹)	Conductivity of UPC-H5a@NH ₃ .H ₂ O (S cm ⁻¹)
30 °C, 95 % R. H.	5.59×10^{-4}	7.00×10^{-3}	1.47×10^{-2}
40 °C, 95 % R. H.	6.98×10^{-4}	9.29×10^{-3}	2.26×10^{-2}
50 °C, 95 % R. H.	8.88×10^{-4}	1.10×10^{-2}	3.19×10^{-2}
60 °C, 95 % R. H.	1.06×10^{-3}	1.27×10^{-2}	5.01×10^{-2}
70 °C, 95 % R. H.	1.36×10^{-3}	1.51×10^{-2}	6.67×10^{-2}
80 °C, 95 % R. H.	1.71×10^{-3}	1.82×10^{-2}	8.68×10^{-2}